

Shape-Responsive Actuator from a Single Layer of a Liquid-Crystal Polymer

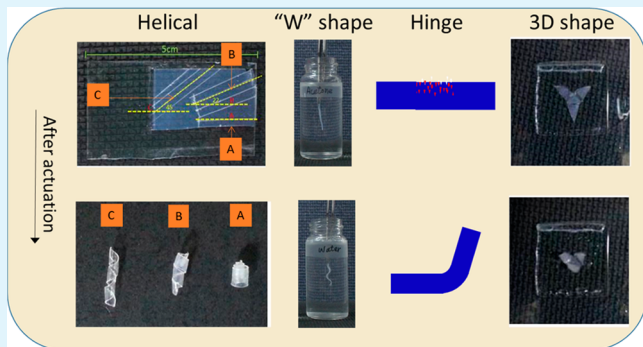
Tahseen Kamal and Soo-young Park*

School of Applied Chemical Engineering, Department of Polymer Science and Engineering, Kyungpook National University, #1370 Sangyuk-dong, Buk-gu, Daegu 702-701, Korea

Supporting Information

ABSTRACT: Actuation of various shape changes, including bending, helical twisting, and reversible hinging, has been achieved from a single-layer sheet of poly(1,4-di(4-(3-acryloyloxypropoxy)benzoyloxy)-2-methylbenzene) [poly(RM257)]. This actuator was developed through photopolymerization of a reactive liquid-crystal (LC) monomer (RM257) mixed with 4-pentyl-4'-cyanobiphenyl (5CB, nematic LC at room temperature) in a planar polyimide-coated LC cell. The UV beam perpendicular to one side of the LC cell produced an asymmetric phase separation between the poly(RM257) network and 5CB that resulted in an asymmetric porous structure along the thickness direction when the 5CB was extracted, in which the UV-exposed surface was pore-free and compact while the opposite surface was highly porous. As a result of this structure, the dry and curled poly(RM257) film exhibits actuation behavior when placed in acetone because of a difference in swelling between the two morphologically different sides, the film UV-exposed and nonexposed sides. The actuation of a three-dimensional tetrahedron (pyramidal) structure is also demonstrated for the first time by using a simple photopatterning technique to selectively control its asymmetric morphology at specific locations.

KEYWORDS: Single layer actuator, photopolymerization, phase separation, three-dimensional actuator, reactive liquid crystal



INTRODUCTION

Research into smart polymers has boomed over the past two decades, leading to the development of not only new active materials but also new actuator systems. Soft and compliant materials have been a particular focus of much of this work, because of the growing interest in developing new solutions for artificial muscles or three-dimensional (3D) objects.^{1,2} Typically, bilayer or multilayer polymer films have been used as actuators, in which bending is achieved by an active stimuli-responsive film imposing stress on the inactive film through a change in volume.

The folding, bending, and twisting of a programmed two-dimensional (2D) stimulus-responsive bilayer sheet can be used to create 3D structures. For instance, Gracias et al. have shown that preassembled nanoscale panels can be transformed into a polyhedral shape by folding.³ However, the tedious steps and metal hinges involved in this create a number of difficulties in terms of practical application. In contrast, polymer-based self-folding 2D sheets are particularly promising for use in biotechnological applications, such as cell encapsulation^{4,5} and the design of biomaterials.⁶ In these and other applications, precise control over the folding and ultimate shape of 3D objects is needed. Previous studies demonstrated pH-responsive,^{7,8} thermally responsive,^{9–11} solvent-responsive,^{12–14} and electrically sensitive active layers,¹⁵ and

patterning of an active layer on passive layers for more complex shape changes.^{12,13} Solvent swelling is typically used because it can provide large, reversible volume changes.^{16,17}

Unlike the stimulus-responsive polymers commonly used in bilayer actuators, monodomain liquid-crystal elastomers (LCEs) used as a single-layer actuator have been demonstrated to exhibit uniaxial elongation, contraction, and bending motion in response to variations in temperature.^{18–22} Furthermore, actuators formed from single-layer LCEs offer the advantage of being impervious to delamination. Typically, LCEs are triggered by physical stimuli such as temperature^{19,21} and light^{23,24} and rarely by chemical stimuli such as humidity.^{25,26} Electric (or magnetic) stimuli have also been utilized by compositing LCEs with inorganic nanomaterials such as nanoparticles, nanowires, and carbon nanotubes.^{16–20} The use of nanoparticles and nanowires has been proven to give additional properties because of the induced alignment of the nanomaterials,²⁷ while carbon nanotubes are capable of triggering actuation by infrared radiation.^{28–31} In a bid to achieve a more complex shape change in LC-based actuators than uniaxial contraction or expansion, a bilayer structure

Received: July 25, 2014

Accepted: September 22, 2014

Published: September 22, 2014

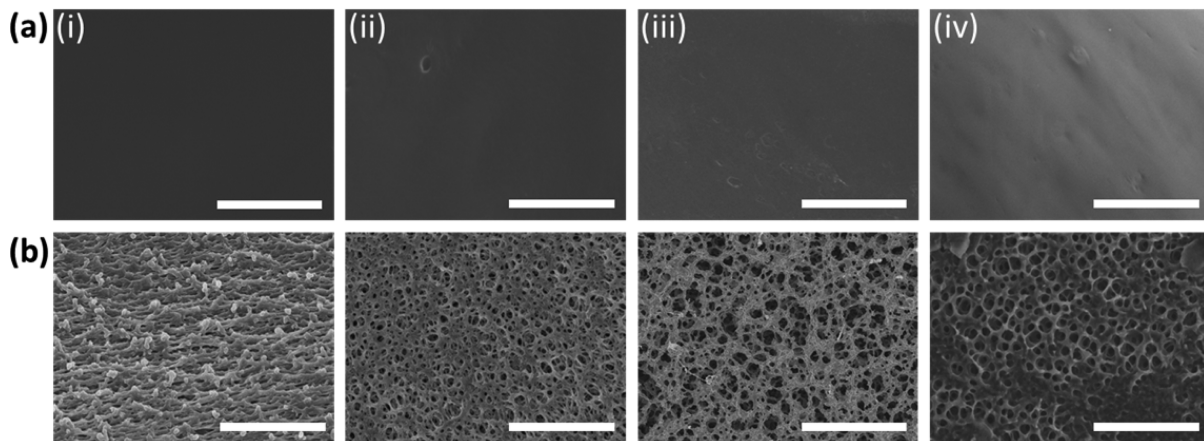


Figure 1. SEM micrographs of (a) UV-exposed and (b) nonexposed sides of poly(RM257) films prepared by photopolymerization of a RM257/5CB ($\phi = 30$ wt %) mixture at UV intensities of (i) 11.6, (ii) 4.8, (iii) 2.1, and (iv) 1.2 mW/cm^2 . All scale bars are 5 μm .

consisting of an active LCE layer deposited on the conductive polymer of a passive non-LCE layer was fabricated.¹³ However, ensuring control over the complex shape of 3D structures and the sensitivity to certain stimuli with such a design requires methods that are both complex and time-consuming.

Although numerous elegant actuator systems have been demonstrated by various academic laboratories, an actuator system based on a monocomponent and single-layer LC actuator has not yet been reported to be transformed into 3D structures. In a previous report,³² a single-layer poly(1,4-di(4-(3-acryloyloxypropoxy)benzoyloxy)-2-methylbenzene) [poly(RM257)] actuator controlled by an asymmetric porous structure along its thickness direction was prepared. In studying the effect of film thickness and the composition of the RM257/5CB mixture on its curvature, we found that a curling and uncurling motion could be created by exposure to alternating water and acetone solvents. In this work, we studied the programming of this actuator film to be transformed into the complex shape including a 3D pyramid structure through directional UV curing and photopatterning of an RM257/4-pentyl-4'-cyanobiphenyl (5CB) mixture in a polyimide (PI)-coated planar LC cell, where RM257 and 5CB are a UV-curable LC diacrylate monomer and orientation-inducible porogen, respectively.

EXPERIMENTAL SECTION

Materials. RM257 (Synthon), 5CB (TCI), acetone (Duksan), ethanol (Duksan), 1-hydroxycyclohexyl phenyl ketone (Sigma-Aldrich), and a polyimide solution (Luxon Aligner, Chisso Corp.) were all used as received. Milli-Q water (resistivity higher than 18.2 Ωcm) was used in all experiments.

RM257/5CB Mixtures and Actuator Film Preparation. RM257/5CB mixtures with various RM257 contents (denoted as ϕ in weight percent) at 10 wt % intervals were prepared by dissolving them in dichloromethane (DCM) containing 1-hydroxycyclohexyl phenyl ketone (photoinitiator, 2 wt % against RM257 monomer). Aluminum foil was wrapped around the vials to protect the mixtures from light, and after being magnetically stirred for 30 min, the DCM was completely evaporated in a vacuum oven at room temperature. The phase behavior of the prepared samples was studied by differential scanning calorimetry and polarized optical microscopy (POM); from that, it was determined that a $\phi = 20\text{--}40$ wt % mixture is most suited to actuator film preparation because of a miscible single phase and a viscosity sufficiently low enough for injection into a LC cell.

To prepare the actuator film, the mixture solutions were injected into planar LC cells fabricated from glass slides. Prior to photo-

polymerization, the filled cells were first inspected by POM under crossed polarizers to confirm the uniform alignment of the RM257/5CB mixtures along the rubbing direction. The cells were then irradiated with a 365 nm ultraviolet (UV) light (Spot UV/Inno cures), with the UV intensity being controlled by varying the distance between the cell and UV source (see Figure SI-1 of the Supporting Information). Following photopolymerization, the cell was opened and immersed in ethanol for 1 h to remove any 5CB from the film. Figure SI-2 of the Supporting Information shows a schematic overview of the entire preparation process.

Measurements. POM images were obtained using an optical microscope (Samwon, LSP-13) under crossed polarizers. Scanning electron microscopy (SEM) (Hitachi, model S-5200 scanning electron microscope) images were obtained at an accelerating voltage of 15 kV; the sample surface was coated with platinum. Actuation of the prepared films was recorded using a Sony Handycam (Sony, model HDR-UX1). Fourier transform infrared (FT-IR) spectra were obtained with a Nicolet-560 spectrometer on potassium bromide (KBr) pellets with a resolution of 4 cm^{-1} . Before being pelleted, samples were washed with ethanol to remove 5CB and dried in a vacuum oven at 40 °C.

RESULTS AND DISCUSSION

Effect of UV Intensity on Film Morphology. The UV intensity during photopolymerization can affect the cross-linking density of the poly(RM257) film, which in turn determines its morphology and actuation. Panels a and b of Figure 1 show SEM micrographs of the UV-exposed and nonexposed sides of poly(RM257) films prepared at UV intensities of 11.6, 4.8, 2.1, and 1.2 mW/cm^2 . This shows that regardless of the UV intensity, the UV-exposed side is smooth, while the nonexposed side is porous. This asymmetric structure results from the competition between polymerization and phase separation, wherein the photoinitiator (1-hydroxycyclohexyl phenyl ketone) is decomposed to benzoyl and cyclohexyl radicals upon exposure to UV light through α -cleavage of the C–C bonds in the RM257 monomer. As a consequence of this, the initial miscible phase becomes increasingly phase-separated as polymerization proceeds. Given that polymerization first occurs at the UV-exposed surface (because of the limited penetrability of UV light into the mixture³³), the phase-separated 5CB is pushed toward the nonexposed side, as this still remains in a miscible state. As polymerization proceeds further, and the concentration of 5CB on the nonexposed side increases, a polymer network is formed with pores at the nonexposed side. Thus, the difference in speed between phase separation and polymerization in the film by UV beam intensity

is one of the main mechanisms for the formation of the asymmetric structure, which caused the difference in swelling, leading to actuating behavior when the film was immersed in the alternatively good and poor solvents (Figure SI-3 of the Supporting Information).

The conversion of the RM257 monomer to poly(RM257) was assessed by FT-IR spectroscopy, the results of which are shown in Figure 2. From this, we see that poly(RM257)

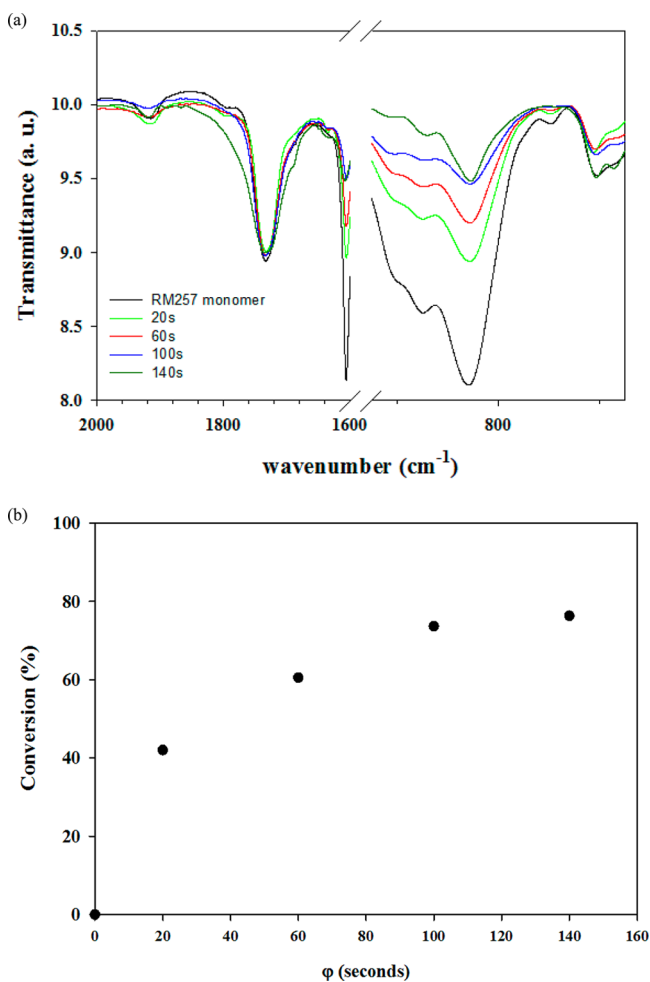


Figure 2. (a) FT-IR spectra of pure RM257 monomer and poly(RM257) films prepared by photopolymerization of a RM257/SCB ($\phi = 30$ wt %) mixture for 20, 60, 100, and 140 s at a constant sample to cell distance of 20 cm (UV intensity of 4.8 mW/cm^2). (b) Conversion of the monomer to poly(RM257) as a function of time (ϕ). All data were calculated from the term $100(1 - R)$, where R is the ratio of FT-IR peak heights at 810 cm^{-1} between time zero and time t .

exhibits peaks at 810 and 1750 cm^{-1} , which correspond to the out-of-plane vibration of the C–H bond of the acrylate group and the C=O stretching vibration of the mesogenic acrylate ester group, respectively.³⁴ The height of the peak at 810 cm^{-1} represents the amount of unreacted RM257 monomer (i.e., the vinyl linkage of the RM257 monomer) and therefore decreases with UV photopolymerization. In contrast, the peak at 1750 cm^{-1} is independent of UV photopolymerization and was therefore used to normalize the spectra. The conversion of monomer to polymer by UV photopolymerization at $\phi = t$ is calculated by $100(1 - R)$, where R is the ratio of the peak heights at 810 cm^{-1} between time zero and time t . Figure 2b

shows the conversion of the monomer to the poly(RM257) as a function of ϕ , in which we see a rapid initial increase followed by saturation at 76% after 100 s. Similar cross-linking densities were achieved by Strapert et al. with the RM257/E7 mixture,³⁴ and thus, photopolymerization was performed for more than 100 s using a sample to UV source distance of 20 cm.

"W" Shape Actuation. In a previous report,³² we found that an asymmetric porous structure causes curling actuation upon immersion in a solvent. Selective UV irradiation of certain areas of the RM257/SCB mixture using photomasks during photopolymerization was therefore used to control the arbitrary shape actuation of the resultant film. To demonstrate model actuation, a simple bar-type photomask was used; however, to also explore the effect of the direction of UV irradiation on the shape of the actuation, a two-step polymerization was conducted. In the first step of photopolymerization, two bar-type photomasks were used at the edges of the LC cell (Figure 3a), whereas the second step used a single photomask in the middle of the inverted cell to ensure UV exposure of all sides of the cell (Figure 3b). This arrangement of photomasks during photopolymerization led to a "W"-shaped poly(RM257) film, which was the result of alternating positive and negative curvatures generated in the UV-exposed outer surface and porous inner surface when it was inserted into water (Figure 3d). However, when the film was inserted into acetone [a good solvent for poly(RM257)], the film became straight (Figure 3c). This actuation is quite unique, because it is something that cannot be achieved in bilayer actuators without the aid of complex patterning.

Helical Coiled Actuation. In addition to the curling and uncurling of the actuator film, actuation into a helically coiled shape was also achieved by cutting the poly(RM257) film at angles of 45° , 22° , and 0° relative to the nematic director (Figure 4a). From the photographs of these same strips after SCB extraction and drying shown in Figure 4b, it is clear that those cut at angles of 45° and 22° adopt a helical coiled shape, whereas a simple curled shape is obtained with the strip cut at an angle of 0° . The cutting angle therefore controls the pitch of the coil in such a way that it is decreased (i.e., a more coiled strip is formed) with an increasing cutting angle. This coiled strip became straight when it was dipped in acetone, as shown in Figure 4c, but reverted to its coiled form when it was dipped in water (Figure 4d). Thus, reversible helical coiling and uncoiling actuation was achieved by simply cutting the poly(RM257) film in the desired direction.

Hinging Actuation. Ensuring a straight surface without curvature during actuation is sometimes necessary to control the various shapes of actuation, so the degree of hinging of two straight surfaces was investigated. Given that the curvature of the film that originated from the asymmetric morphology induced between its UV-exposed and nonexposed sides, it can be prevented by using an Al foil UV reflector to irradiate simultaneously both sides of the LC cell, as shown in Figure 5. In this way, a two-step photopolymerization of a RM257/SCB mixture ($\phi = 20$ wt %) in the planar LC cell was used to make a hinge. The first photopolymerization was performed using a UV source to sample a distance of 40 cm and the UV reflector positioned on the other side of the cell, with a 2 mm wide photomask positioned beneath and above the cell and aligned with its center. The second photopolymerization omitted the UV reflector with a negative photomask and was conducted at UV source to sample distances ranging from 10 to 40 cm.

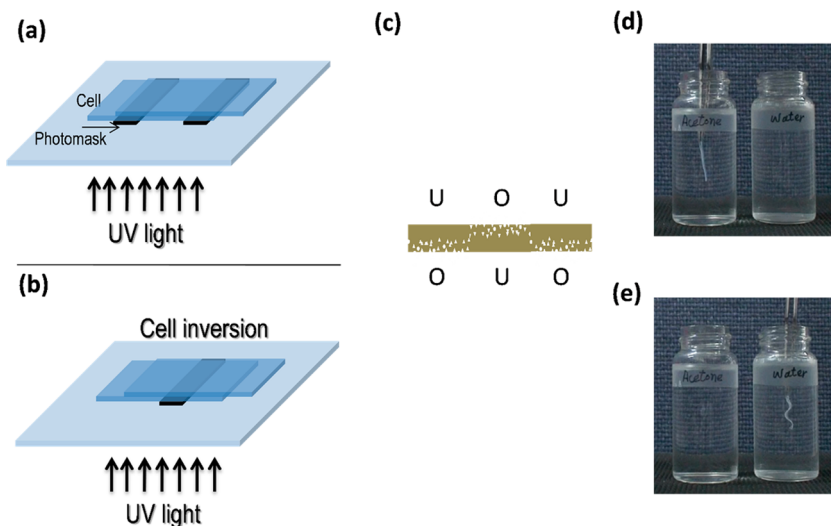


Figure 3. “W” shape actuation of a poly(RM257) film prepared by a two-step photopolymerization: (a) first-step photopolymerization using bar photomasks on the edges of a planar LC cell and (b) second-step photopolymerization using a bar photomask at the center of the reversed planar LC cell (the UV source is positioned underneath the LC cell in both cases). (c) Schematic diagram showing the cross section of the resultant poly(RM257) film, where U and O are the UV-exposed and opposite (nonexposed) sides, respectively. Fabricated film in (d) acetone and (e) water, showing the “W” shape actuation that is generated by alternately dipping in good (acetone) and poor (water) solvents.

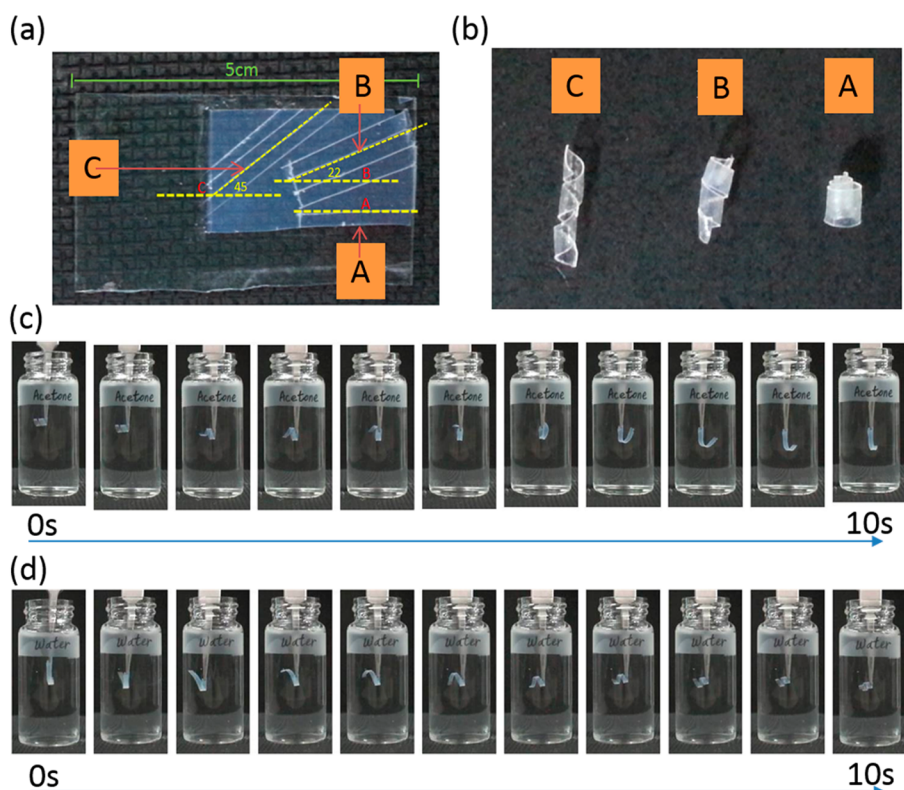


Figure 4. (a) Digital photographs of an actuator film made at $\phi = 20$ wt % prior to 5CB extraction, from which three strips (A–C) were cut at angles of 0° , 22° , and 45° relative to the rubbing (horizontal) direction. (b) Coiled strips A–C after 5CB extraction in ethanol and drying. (c) Uncoiling in acetone and (d) coiling in water of an A strip.

In the photographs of the poly(RM257) film in water shown in Figure 5, it is clearly evident that the straight surface becomes more hinged as the UV intensity increases. The degree of bending, as measured between the two straight planes, was found to be 97° , 89° , 79° , and 76° with UV intensities of 11.6 , 4.8 , 2.1 , and 1.2 mW/cm^2 , respectively. This result indicates that the degree of bending decreased until it

reached $\sim 2.1 \text{ mW}/\text{cm}^2$ as the UV intensity increased and then was saturated. These straight surfaces were obtained by the use of the UV reflector in the first stage of polymerization to create a homogeneous structure inside the LC film. The hinge, located at the position of the photomask in the first step, represents an asymmetrically structured area created by directional UV photopolymerization. The bending angle decreases with a

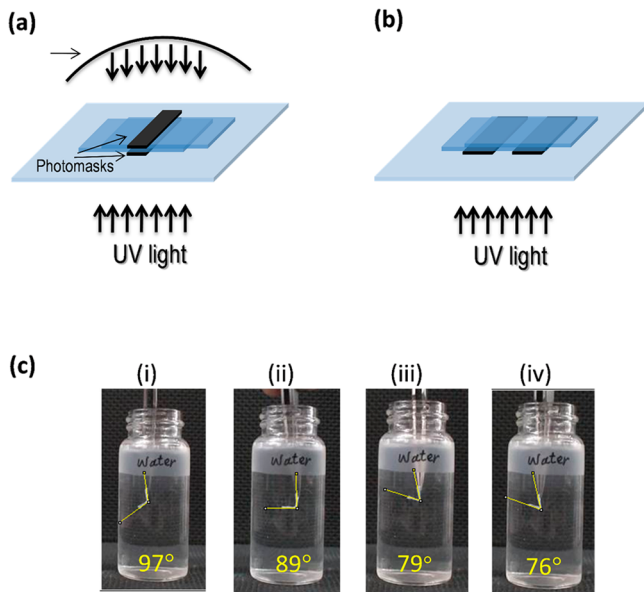


Figure 5. Two-step photopolymerization of the RM257/5CB mixture ($\phi = 20$ wt %) in the planar LC cell for hinging actuation. (a) The first photopolymerization was performed at the UV source to sample a distance of 40 cm with the UV reflector at the other side of the UV source and a 2 mm wide photomask beneath and above the cell at the center. (b) Second photopolymerization without the UV reflector at different UV intensities. (c) Photographs of hinged poly(RM257) films in water prepared at sample to UV source distances of (i) 10 (11.6), (ii) 20 (4.8), (iii) 30 (2.1), and (iv) 40 (1.2) cm (the numbers in parentheses represent the measured UV intensities in milliwatts per square centimeter).

decrease in the UV intensity. This means that the slower rate of photopolymerization due to a decrease in UV intensity results in a different thickness of the porous part and the condensed nonporous part in the area of asymmetric structure along the film thickness, and therefore the amount of hinge. Such results

indicate that a controlled amount of hinging can be created between straight planes through the use of a UV reflector, UV intensity, and narrow photomasks.

3D Actuation. Complex 3D structure actuation based on non-LC systems has been explored by several scientists;^{2,12,35} however, LC-based systems have been mostly limited to uniaxial elongation–contraction or bending–unbending systems except for a few in which different monomer mixtures were used. Furthermore, 3D structure actuation with a single-layer structure from a single monomer has not yet been reported. Recently, Verduzco et al. were able to utilize an LCE-based bilayer system for the fabrication of a shape-responsive actuator based on an LCE/polystyrene (PS) sheet, which was shaped into a flowerlike 3D structure by a nematic to isotropic transition.³⁶ As described in the previous section, the first step to make a 3D convertible sheet of a poly(RM257) film was the creation of hinged actuation. Using this, line photomasks of an equilateral triangle (1 mm line width, 3 mm side length) and an equivalent negative mask were prepared on a transparent PET film by an inkjet printer (see Figure SI-4 of the Supporting Information). During the first photopolymerization step (Figure 6), the equilateral triangle photomasks were placed above and below the cell, thereby preventing UV polymerization of the RM257 monomers in the same location on both sides of the LC cell. A UV source to sample distance of 30 cm (2.1 mW/cm^2) was used, with a UV reflector placed on the other side of the LC cell to ensure an equal dose of UV light on both sides. In the second photopolymerization step (Figure 6b), the remaining unpolymerized mixture was photopolymerized by using the negative photomask without a UV reflector, and with a UV source to sample distance of 20 cm (4.8 mW/cm^2). The resulting photopolymerized 2D sheet was then cut into a three-arm star shape to achieve the regular tetrahedron structure actuation shown in Figure 6c, in which no bending of the hinged part is observed upon immersion in acetone due to photopolymerization having been performed in a similarly good solvent (as discussed for curling actuation).

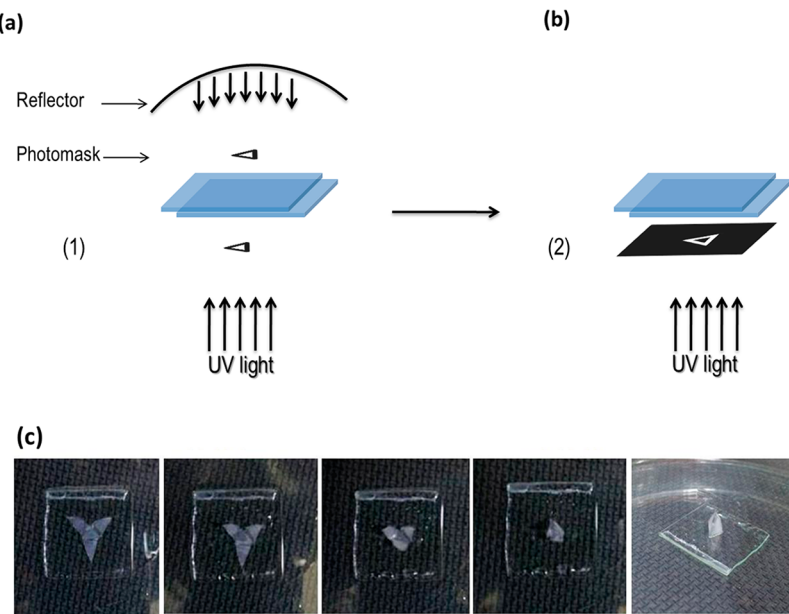


Figure 6. Photopolymerization steps for the preparation of the programmable 2D sheet. The film was prepared using (a) triangular positive photomasks below and above the cell with a UV reflector in the first step and (b) a negative photomask without a UV reflector in the second step. (c) Photographs of a 2D poly(RM257) film showing 3D actuation of a pyramidal structure during evaporation of acetone.

When this system was kept in open air to let the acetone freely evaporate, the hinged parts of the three sides of the triangle increasingly bent to form a pyramidal structure, which was subsequently returned to a flat 2D structure when acetone was dropped on the structure. The required 51° angle in the closed pyramidal structure was achieved using a thin cell (130 μm) compared to that used in hinging actuation where an 89° bending angle was achieved using the same UV beam intensity of 4.8 mW/cm². As far as we are aware, this is the first such demonstration of a single-layer actuator programmed to adopt a 3D shape.

The actuation in this study was obtained by a combination of the morphological control and axial molecular orientation. This approach has merits over the molecular orientation control with monomers having twisted and splayed directors because the fabrication setup is simple and requires only a common LC diacrylate monomer. Also, the curing of the LC monomer mixture in the nematic state requires heating or addition of extra monomers for lowering the T_{ni} ; however, adopting the current approach of polymerization-induced phase separation eliminates the process of heating.

CONCLUSION

A single-layer LC cross-linked actuator was successfully fabricated using a simple method that entails the directional UV curing of a RM257/SCB mixture in a planar LC cell. The fabricated films had an asymmetric porous structure along the film thickness direction, as well as an axial orientation along the rubbing direction. This unique structure induced curling actuation in the film along the rubbing direction upon immersion in water because of the difference in swelling between the UV-exposed and nonexposed sides. The arbitrary shape of actuation could be programmed through controlled patterning with photomasks, with "W"-shaped curling and helical coiling being demonstrated with simple alternating patterns and cutting the film along a desired direction, respectively. A hinged flat surface was also obtained by controlling the UV intensity with positive and negative photomasks. Finally, an arbitrary 3D structure actuation was demonstrated using a pyramidal structure formed from a single-layer LC film, which we believe has great potential to provide the basis for further development of actuation.

ASSOCIATED CONTENT

Supporting Information

LC cell fabrication, control of UV intensity, schematic for actuator film preparation, and preparation of the photomasks for the pyramidal-responsive film. This material is available free of charge via the Internet at <http://pubs.acs.org>.

AUTHOR INFORMATION

Corresponding Author

*E-mail: psy@knu.ac.kr

Notes

The authors declare no competing financial interest.

ACKNOWLEDGMENTS

This work was supported by the National Research Foundation of Korea (NRF-2011-0020264).

REFERENCES

- (1) Kim, S. J.; Spinks, G. M.; Prosser, S.; Whitten, P. G.; Wallace, G. G.; Kim, S. I. Surprising shrinkage of expanding gels under an external load. *Nat. Mater.* **2006**, *5* (1), 48–51.
- (2) Stoychev, G.; Zakharchenko, S.; Turcaud, S.; Dunlop, J. W. C.; Ionov, L. Shape-Programmed Folding of Stimuli-Responsive Polymer Bilayers. *ACS Nano* **2012**, *6* (5), 3925–3934.
- (3) Gracias, D. H.; Kavthekar, V.; Love, J. C.; Paul, K. E.; Whitesides, G. M. Fabrication of Micrometer-Scale, Patterned Polyhedra by Self-Assembly. *Adv. Mater. (Weinheim, Ger.)* **2002**, *14* (3), 235–238.
- (4) Stoychev, G.; Puretskiy, N.; Ionov, L. Self-folding all-polymer thermoresponsive microcapsules. *Soft Matter* **2011**, *7* (7), 3277–3279.
- (5) Zakharchenko, S.; Puretskiy, N.; Stoychev, G.; Stamm, M.; Ionov, L. Temperature controlled encapsulation and release using partially biodegradable thermo-magneto-sensitive self-rolling tubes. *Soft Matter* **2010**, *6* (12), 2633–2636.
- (6) Zakharchenko, S.; Sperling, E.; Ionov, L. Fully Biodegradable Self-Rolled Polymer Tubes: A Candidate for Tissue Engineering Scaffolds. *Biomacromolecules* **2011**, *12* (6), 2211–2215.
- (7) Bassik, N.; Abebe, B. T.; Laflin, K. E.; Gracias, D. H. Photolithographically patterned smart hydrogel based bilayer actuators. *Polymer* **2010**, *51* (26), 6093–6098.
- (8) Kelby, T. S.; Huck, W. T. S. Controlled Bending of Microscale Au–Polyelectrolyte Brush Bilayers. *Macromolecules* **2010**, *43* (12), 5382–5386.
- (9) Behl, M.; Razzaq, M. Y.; Lendlein, A. Multifunctional Shape-Memory Polymers. *Adv. Mater. (Weinheim, Ger.)* **2010**, *22* (31), 3388–3410.
- (10) Simpson, B.; Nunnery, G.; Tannenbaum, R.; Kalaitzidou, K. Capture/release ability of thermo-responsive polymer particles. *J. Mater. Chem.* **2010**, *20* (17), 3496–3501.
- (11) Ziolkowski, B.; Diamond, D. Thermoresponsive poly(ionic liquid) hydrogels. *Chem. Commun.* **2013**, *49* (87), 10308–10310.
- (12) Jeong, K.-U.; Jang, J.-H.; Kim, D.-Y.; Nah, C.; Lee, J. H.; Lee, M.-H.; Sun, H.-J.; Wang, C.-L.; Cheng, S. Z. D.; Thomas, E. L. Three-dimensional actuators transformed from the programmed two-dimensional structures via bending, twisting and folding mechanisms. *J. Mater. Chem.* **2011**, *21* (19), 6824–6830.
- (13) Kelby, T. S.; Wang, M.; Huck, W. T. S. Controlled Folding of 2D Au–Polymer Brush Composites into 3D Microstructures. *Adv. Funct. Mater.* **2011**, *21* (4), 652–657.
- (14) Bumbu, G.-G.; Wolkenhauer, M.; Kircher, G.; Gutmann, J. S.; Berger, R. Micromechanical Cantilever Technique: A Tool for Investigating the Swelling of Polymer Brushes. *Langmuir* **2007**, *23* (4), 2203–2207.
- (15) Smela, E.; Inganäs, O.; Lundström, I. Controlled Folding of Micrometer-Size Structures. *Science* **1995**, *268* (5218), 1735–1738.
- (16) Chen, X.; Tsujii, K. A Novel Hydrogel Showing Super-Rapid Shrinking but Slow Swelling Behavior. *Macromolecules* **2006**, *39* (25), 8550–8552.
- (17) Imran, A. B.; Seki, T.; Ito, K.; Takeoka, Y. Poly(N-isopropylacrylamide) Gel Prepared Using a Hydrophilic Polyrotaxane-Based Movable Cross-Linker. *Macromolecules* **2010**, *43* (4), 1975–1980.
- (18) Yang, H.; Liu, M.-X.; Yao, Y.-W.; Tao, P.-Y.; Lin, B.-P.; Keller, P.; Zhang, X.-Q.; Sun, Y.; Guo, L.-X. Polysiloxane-Based Liquid Crystalline Polymers and Elastomers Prepared by Thiol-Ene Chemistry. *Macromolecules* **2013**, *46* (9), 3406–3416.
- (19) Sawa, Y.; Urayama, K.; Takigawa, T.; DeSimone, A.; Teresi, L. Thermally Driven Giant Bending of Liquid Crystal Elastomer Films with Hybrid Alignment. *Macromolecules* **2010**, *43* (9), 4362–4369.
- (20) Qin, H.; Mather, P. T. Combined One-Way and Two-Way Shape Memory in a Glass-Forming Nematic Network. *Macromolecules* **2009**, *42* (1), 273–280.
- (21) Urayama, K. Selected Issues in Liquid Crystal Elastomers and Gels. *Macromolecules* **2007**, *40* (7), 2277–2288.
- (22) Bispo, M.; Guillou, D.; Donnio, B.; Finkelmann, H. Main-Chain Liquid Crystalline Elastomers: Monomer and Cross-Linker Molecular

Control of the Thermotropic and Elastic Properties. *Macromolecules* **2008**, *41* (9), 3098–3108.

(23) Yu, H.; Ikeda, T. Photocontrollable Liquid-Crystalline Actuators. *Adv. Mater. (Weinheim, Ger.)* **2011**, *23* (19), 2149–2180.

(24) de Haan, L. T.; Sánchez-Somolinos, C.; Bastiaansen, C. M. W.; Schenning, A. P. H. J.; Broer, D. J. Engineering of Complex Order and the Macroscopic Deformation of Liquid Crystal Polymer Networks. *Angew. Chem., Int. Ed.* **2012**, *51* (50), 12469–12472.

(25) Broer, D. J.; Bastiaansen, C. M. W.; Debije, M. G.; Schenning, A. P. H. J. Functional Organic Materials Based on Polymerized Liquid-Crystal Monomers: Supramolecular Hydrogen-Bonded Systems. *Angew. Chem., Int. Ed.* **2012**, *51* (29), 7102–7109.

(26) Harris, K. D.; Bastiaansen, C. W. M.; Lub, J.; Broer, D. J. Self-Assembled Polymer Films for Controlled Agent-Driven Motion. *Nano Lett.* **2005**, *5* (9), 1857–1860.

(27) Domenici, V.; Zupančič, B.; Laguta, V. V.; Belous, A. G.; Vyunov, O. I.; Remškar, M.; Zalar, B. t. PbTiO₃ Nanoparticles Embedded in a Liquid Crystalline Elastomer Matrix: Structural and Ordering Properties. *J. Phys. Chem. C* **2010**, *114* (24), 10782–10789.

(28) Ahir, S. V.; Terentjev, E. M. Photomechanical actuation in polymer-nanotube composites. *Nat. Mater.* **2005**, *4* (6), 491–495.

(29) Sun, X.; Wang, W.; Qiu, L.; Guo, W.; Yu, Y.; Peng, H. Unusual Reversible Photomechanical Actuation in Polymer/Nanotube Composites. *Angew. Chem., Int. Ed.* **2012**, *51* (34), 8520–8524.

(30) Pradhan, B.; Kohlmeyer, R. R.; Setyowati, K.; Owen, H. A.; Chen, J. Advanced carbon nanotube/polymer composite infrared sensors. *Carbon* **2009**, *47* (7), 1686–1692.

(31) Marshall, J. E.; Ji, Y.; Torras, N.; Zinoviev, K.; Terentjev, E. M. Carbon-nanotube sensitized nematic elastomer composites for IR-visible photo-actuation. *Soft Matter* **2012**, *8* (5), 1570–1574.

(32) Kamal, T.; Park, S.-Y. A liquid crystal polymer based single layer chemo-responsive actuator. *Chem. Commun.* **2014**, *50* (16), 2030–2033.

(33) van Oosten, C. L.; Bastiaansen, C. W. M.; Broer, D. J. Printed artificial cilia from liquid-crystal network actuators modularly driven by light. *Nat. Mater.* **2009**, *8* (8), 677–682.

(34) Stapert, H. R.; del Valle, S.; Versteegen, E. J. K.; van der Zande, B. M. I.; Lub, J.; Stallinga, S. Photoreplicated Anisotropic Liquid-Crystalline Lenses for Aberration Control and Dual-Layer Readout of Optical Discs. *Adv. Funct. Mater.* **2003**, *13* (9), 732–738.

(35) Martinez, R. V.; Fish, C. R.; Chen, X.; Whitesides, G. M. Elastomeric Origami: Programmable Paper-Elastomer Composites as Pneumatic Actuators. *Adv. Funct. Mater.* **2012**, *22* (7), 1376–1384.

(36) Agrawal, A.; Yun, T.; Pesek, S. L.; Chapman, W. G.; Verdúzco, R. Shape-responsive liquid crystal elastomer bilayers. *Soft Matter* **2014**, *10* (9), 1411–1415.